Searching for Y dwarfs at the faint limits of WISE

M. Gromadzki[1,2], D. Pinfield[3], S. K. Leggett[4], J. Gomes[3], A. C. Day-Jones[3], N. Lodieu[5,6], M. T. Ruiz[7], R. Kurtev[2,1], N. J. Cook[3], C. V. Morley[8], M. S. Marley[9], F. Marocco[3], Y. Beletsky[10], V. D. Ivanov[11], J.C. Beamín[12,11,1], B. Burningham[10,3], T. Cattermole[3], C. Cardoso[13], J. Faherty[14], S. Littlefair[15], R. Smart[13], M. Irwin[16], J. R. A. Clarke[2], L. Smith[3], P. W. Lucas[3], M. C. Gálvez-Ortiz[17], J. Frith[18], J. S. Jenkins[7], H. R. A. Jones[3], R. Rebolo[5,6], V. J. S. Béjar[5,6], B. Gauza[5,6] and Z. Zhang[5,6]

[1]Millenium Institute of Astrophysics, Chile
[2]Universidad de Valparaíso, Chile
[3]University of Hertfordshire, UK
[4]Gemini Observatory, USA
[5]Insituto de Astrofísica de Canarias, Spain
[6]Universidad La Lagna, Spain
[7]Universidad de Chile
[8]University of California, Santa Cruz, USA
[9]NASA Ames Research Center, USA
[10]Las Campanas Observatory, Chile
[11]European Southern Observatory
[12]Pontificia Universidad Católica de Chile
[13]Instituto Nazionale di Astrofisica, Torino, Italy
[14]Carnegie Institute of Washington, USA
[15]University Sheffield, UK
[16]Institute of Astronomy, Cambridge, UK
[17]Centro de Astrobiología, Madrid, Spain
[18]Jacobs Technology, Houston, USA

INTRODUCTION

WISE is undoubtedly one of the most successful facility ever used in the brown dwarfs research. It has found plenty of late T dwarfs and identified first Y dwarfs (e.g. Cushing et al. 2011; Kirkpatrick et al. 2011; Tinney et al. 2012). Its pass-bands are optimized to detect such cool objects. In particular *W*1 covers a deep CH4 absorption band in the spectra of cool brown dwarfs with *W*2 covering a spectral region of relatively low opacity. They present extremely red colours (*J*−*W*2 > 4) and *J*−*H* indicate a reverse of the previously known colour trend of dwarfs (for bluer *J*−*H*), showing collapse in the near-IR flux compare to that in ∼ 5 microns peak.

SEARCH METHOD

The search method identified WISE All-Sky sources detected in the *W*2-band only, and probed down to low signal-to-noise levels S/N > 8, targeting objects with faint *W*2 magnitudes and red *W*1−*W*2 colour. Spurious sources were removed using database selection criteria defined through analysis of a control sample comprising isolated pointlike, non-variable, non-moving sources from the SDSS. A brief summary of the selection and rejection criteria is given below (more details see (Pinfield et al. 2014a):

• Select sources only detected in the *W*2 band with S/N≥8. Require at least 8 individual exposures (in all bands) covering the sky position.

• The line of sight extinction must be *Av* < 0.8 to remove reddened contamination.

• Reject non-point-like sources for which the reduced χ2 of the *W*2 profile fit photometry was >1.2.

• Reject sources for which the scatter in the multiple measurement photometry was higher than expected from the integrated flux uncertainty.

• Reject sources for which the number of detections in the individual *W*2 rames was less than expected.

• Reject faint sources (*W*2 signal-to-noise from 8-10) within extended bright star halo regions, by comparing with 2MASS point-source-catalogue positions (see figure 2 of Pinfield et al. 2014a).

• Select final candidates by visual inspection, rejecting artefacts, resolved extended structures (e.g. nebulosity and galaxies), badly blended sources, and sources with visual *W*1, *W*3 or *W*4 detections.

We identify 158 candidate late objects. Twenty eight of these sources are previously identified T5-Y dwarfs from the literature (Burningham et al. 2010; Kirkpatrick et al. 2012; Lodieu et al. 2012). The dominant magnitude range for the new sample is *W*2 = 15−16, where we find 116 sources. Our sample also contains 25 sources fainter than *W*2 = 16 (see Figure 1.).

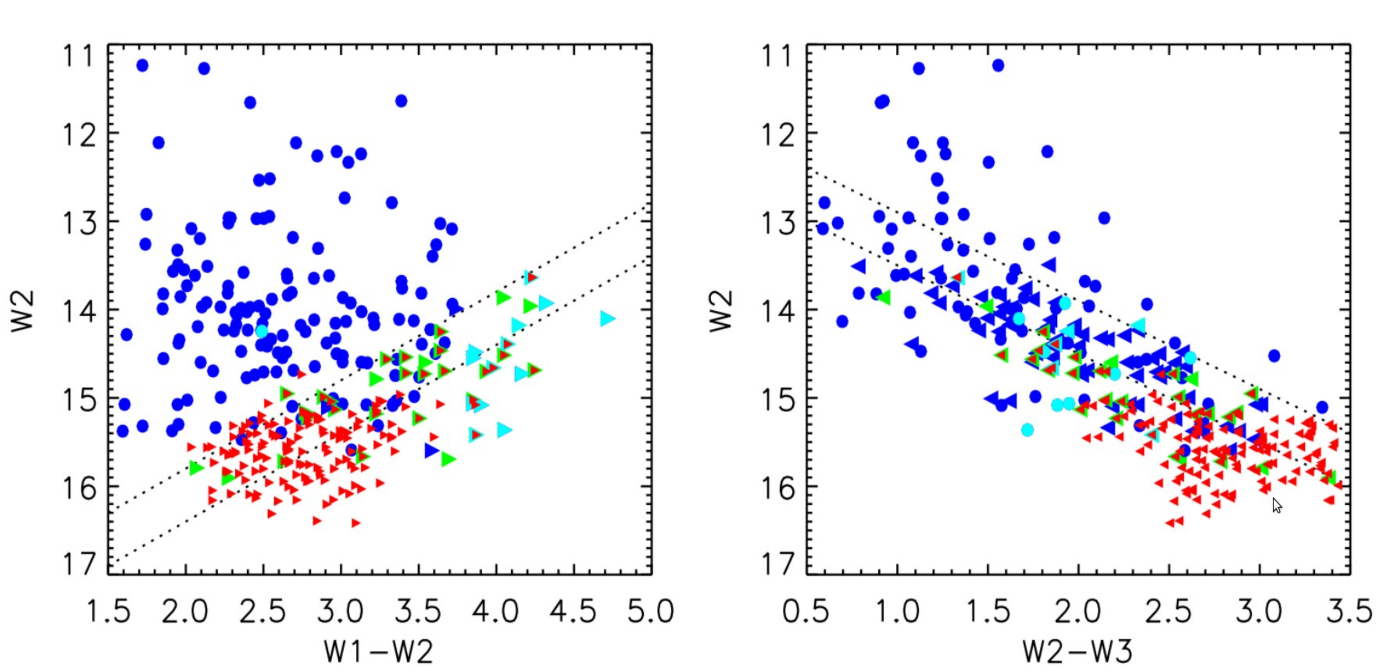

Figure 1: *W*1-*W*2 versus *W*2 colour-magnitude diagram. Our new sample is shown in red. Discoveries from the WISE team's programme are blue, except when their sources are only detected in *W*2 (green) or are Y dwarfs (cyan). Triangles point towards an increasing or decreasing colour for lower or upper limit colours respectively. Our new sample dominates in the *W*2=15-16 range, and has limit colours consistent with late T or Y dwarfs.

FOLLOW-UP

We follow-up our WISE candidates with J-band imaging initially using survey data (UKIDSS, UHS, VISTA) as well as targeted observations (using Magellan, Gemini North and South, UKIRT and NTT). This allows us to identify mid T dwarfs and spurious highly reddened sources with *J*−*W*2 < 4 (accounting for ∼20% of our sample). *J*-detected candidates with redder *J*−*W*2 > 4 may be T8 or later or later (e.g. fig 7 of Kirkpatrick et al. 2011). For these we measure additional photometry in the *H*-band and/or *J*3+*J*2-bands (Magellan filters designed to measure the strength of methane absorption in the J-band). We then assess *J*−*H* colour which is blue for most Y dwarfs (e.g. fig 7 of Kirkpatrick et al. 2012), and/or *J*3−*J*2 which should be < -0.5 for late T and Y dwarfs (see Tinney et al. 2012).

Proper motion measurements are also obtained where a suitable epoch difference is available (see Fig 2.). Contamination from galaxies and young stellar objects is thus identified (∼20% of sample), with good candidates fed through for spectroscopy (∼10% of sample) using FIRE/Magellan and GNIRS + FLAMINGOS2/Gemini. We can also obtain near-infrared spectroscopy to *J*∼22 or *J*−[4.5] = 6−7 (i.e. for typical early Y dwarfs). An example spectrum (of our first Y dwarf) is shown on Fig 3. We find that ∼ 50% of our sample are undetected in the initial J-band imaging, and these (along with confirmed T8–Y dwarfs) are targeted by our Spitzer follow-up.

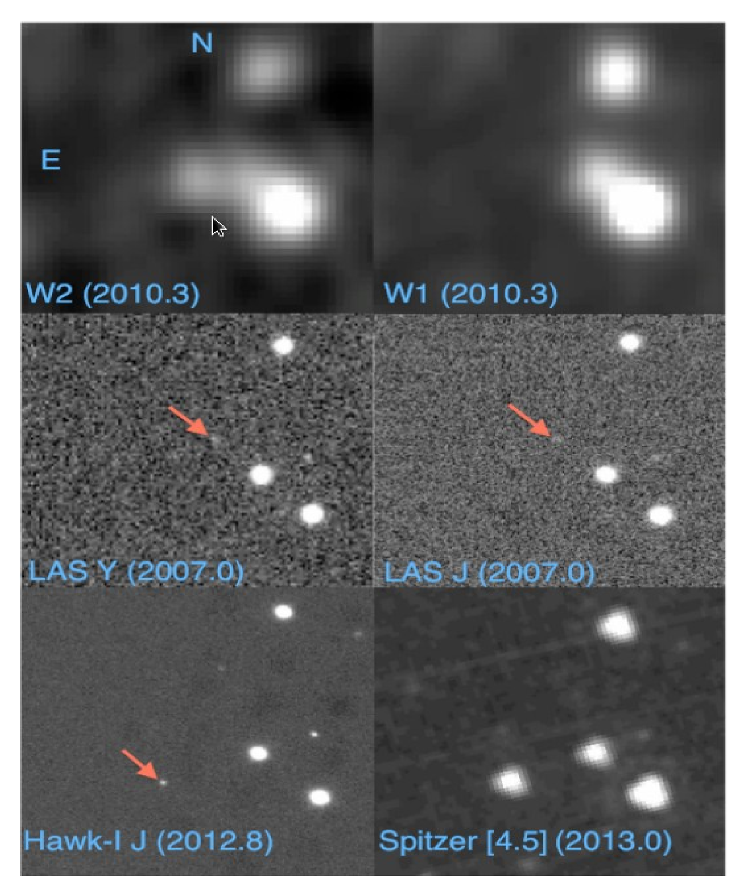

Figure 2: Multiband images of WISE 0833+0052. Each image is 1 arcmin on the side. The top two plots are WISE *W*2- and *W*1-band images on the left and right, respectively, with WISE 0833+0052 in the centre. The middle two plots show the UKIDSS *Y*- and *J*-band images from 2006.95. The bottom two plots show the VLT Hawk-I *J* image from 2012.8 and the Spitzer [4.5] image from 2013.0. The high proper motion near-infrared counterpart is indicated in each image by a red arrow, and has moved by 10.4 arcsec across the near-infrared epochs.

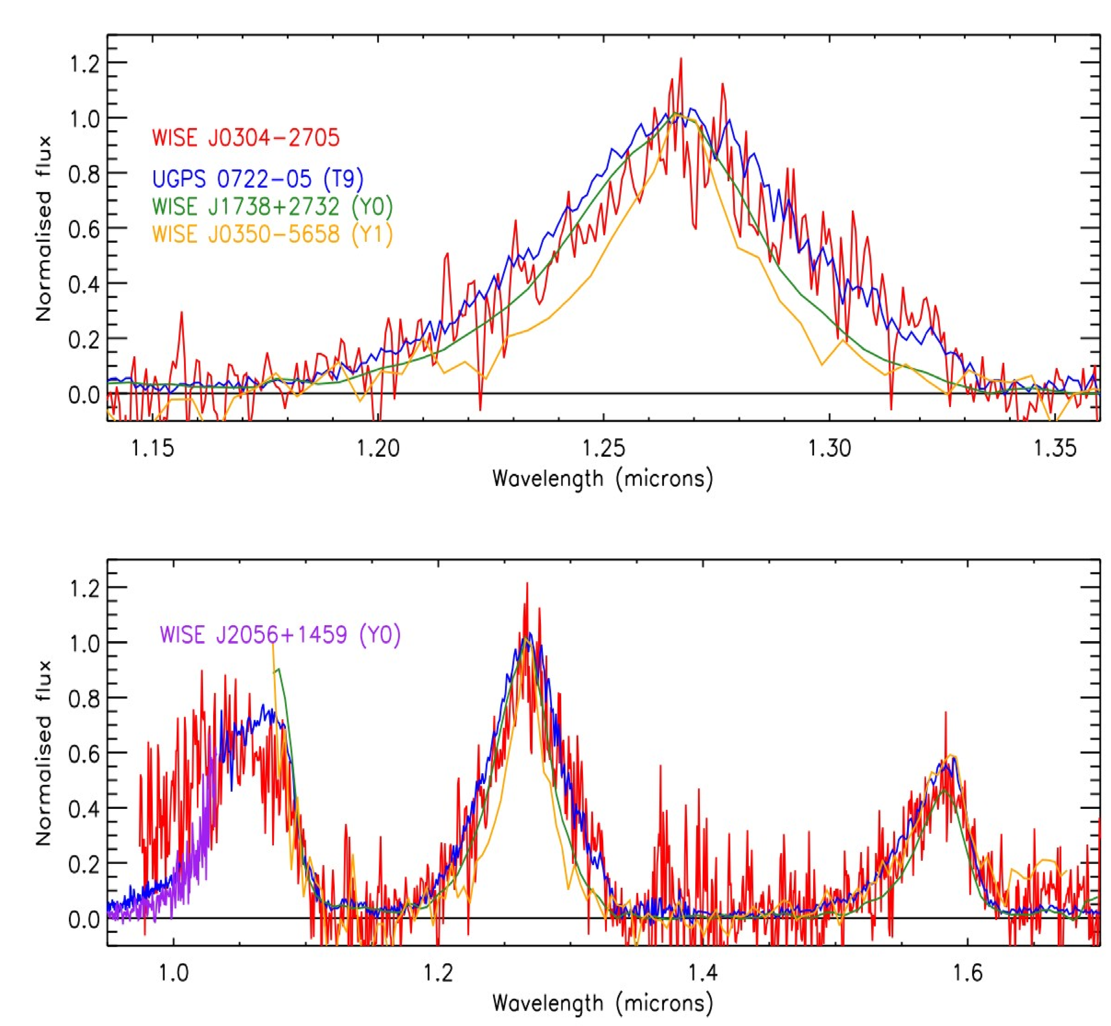

Figure 3: The near-IR Gemini South Flamingos-2 spectrum of WISE J0304-2705. The top plot shows the J-band region, and the lower plot the full Y JH range. Several spectra are over-plotted for comparison: UGPS 0722-05 (T9), WISE J1738+2732 (Y0), WISE J0350-5658 (Y1), and red-optical WISE J2056+1459 (Y0). All spectra are normalised to an average of unity from 1.265-1.270 μm. Plot taken from (Pinfield et al. 2014b).

SUMMARY

Our deep search is probing a larger volume for unusual rare T dwarfs such as the high velocity population. To date we have spectroscopically confirmed seven T8-Y0 dwarfs. This includes one Y dwarf, which shows peculiar spectral morphology and could be the first Y0 dwarf that is a member of the old disk (Pinfield et al. 2014b). We have also published a T8 and a T9 with kinematics of the thick-disk/halo (see Fig 4.; Pinfield et al. 2014a), and have spectroscopically confirmed 3 additional T8-9 dwarfs one of which is the most K-band suppressed late T dwarf yet found, and another also has thick-disk/halo kinematics (Pinfield et al. and Gromadzki et al. in prep). In addition we have 3 strong photometric candidates waiting for spectroscopic follow-up.

We are also creating a new expanded candidate sample using an improved version of our original selection method, which we now apply to the AllWISE database. This method is sensitive to moving as well as stationary objects, and reaches down to significantly fainter limits than have been previously attempted. As the WISE mission continues, and new data products emerge, the sensitivity of our new method will continue to improve.

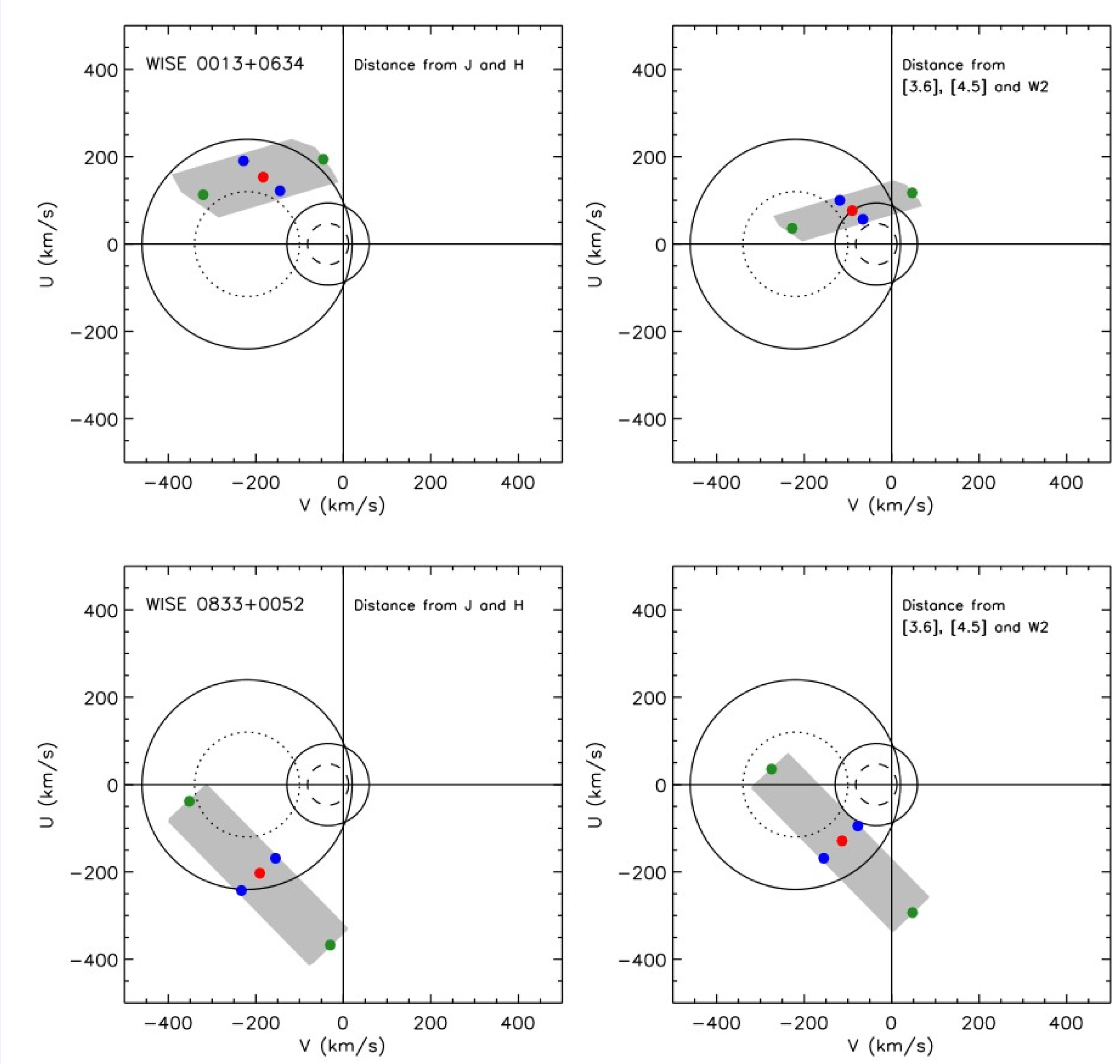

Figure 4: UV space motion plots for WISE 0013+0634 and WISE 0833+0052. Uncertainties in measured proper motion and estimated distance have been accounted for, as well as a possible range in RV from −250 to +250 km/s . In the left-hand plots distances were estimated using *JH* brightness, while in the right-hand plots they were estimated using (relatively overluminous) mid-infrared brightness. Old disc and halo velocity dispersions (1 and 2σ as dashed/dotted and solid lines, respectively) are also shown from Chiba & Beers (2000).

Acknowledgments: Support for MG is provided by the Ministry of Economy, Development, and Tourisms Millennium Science Initiative through grant IC12009, awarded to The Millennium Institute of Astrophysics, Joined Committee ESO and Government of Chile 2014 and FONDECYT grants No. 1120601.

REFERENCES

Burningham, B., Pinfield, D. J., Lucas, P. W., et al. 2010, MNRAS, 406, 1885
Chiba & Beers 2000, AJ, 119, 2843
Cushing, M. C., Kirkpatrick, J. D., Gelino, C. R., et al. 2011, ApJ, 743, 50
Kirkpatrick, J. D., Cushing, M. C., Gelino, C. R., et al. 2011, ApJS, 197, 19
Kirkpatrick, J. D., Gelino, C. R., Cushing, M. C., et al. 2012, ApJ, 753, 156
Lodieu, N., Burningham, B., Day-Jones, A., et al. 2012, A&A, 548, AA53
Pinfield, D. J., Gomes, J., Day-Jones, A. C., et al. 2014a, MNRAS, 437, 1009
Pinfield, D. J., Gromadzki, M., Leggett, S. K., et al. 2014b, MNRAS, 444, 1931
Tinney, C. G., Faherty, J. K., Kirkpatrick, J. D., et al. 2012, ApJ, 759, 60